Inorg. Chem. **2002**, *41*, 3230–3238

Magnetic Molecular Conductors Based on BETS Molecules and Divalent Magnetic Anions [BETS = Bis(ethylenedithio)tetraselenafulvalene]

Emiko Fujiwara,[†,‡] Victor Gritsenko,[†,§] Hideki Fujiwara,[†] Itaru Tamura,[†] Hayao Kobayashi,*[,†] Madoka Tokumoto,[||] and Akiko Kobayashi[‡]

Institute for Molecular Science, Myodaiji, Okazaki 444-8585, Japan, Research Centre for Spectrochemistry, Graduate School of Science, The University of Tokyo, Hongo, Bunkyo-ku, Tokyo 113-0033, Japan, Institute of Problems of Chemical Physics, RAS, Chernogolovka, Moscow Region 142432, Russia, and National Institute of Advanced Industrial Science and Technology, Umezono, Tsukuba 305-8568, Japan

Received November 13, 2001

Several conducting salts based on BETS [where BETS = bis(ethylenedithio)tetraselenafulvalene] molecules and divalent magnetic anions such as the $(CoCl_4)^{2-}$, $(CoBr_4)^{2-}$, and $(MnBr_4)^{2-}$ were prepared. Electrocrystallization by using the $(CoCl_4)^{2-}$ anion gave two kinds of crystals. Block-shaped crystals were cleared to be $(BETS)_2CoCl_4$, which is an insulator with the high-spin state of cobalt 3d spin. On the other hand, the X-ray crystal structure analysis of a plate-shaped crystal of the $(CoCl_4)^{2-}$ salt revealed the system to be κ-$(BETS)_4CoCl_4(EtOH)$, which is metallic down to 0.7 K. The electronic band structure calculation gave a typical two-dimensional cylindrical Fermi surface. However, there is only very weak antiferromagnetic interaction between the $S = {}^3/_2$ cobalt 3d spins because of its anion–solvent-intermingled layer structure. On the other hand, the electrocrystallization by using the $(MnBr_4)^{2-}$ anion yielded the plate-shaped black crystals of the $(MnBr_4)^{2-}$ salt. Crystal structure analysis of the $(MnBr_4)^{2-}$ salt showed that the salt is θ-$(BETS)_4MnBr_4(EtOH)_2$ with alternating donor and anion–solvent mixed layers. The stacking direction in one donor layer is perpendicular to those of the neighboring layers. The electrical and magnetic properties of the θ-$(BETS)_4MnBr_4(EtOH)_2$ salt showed the metallic behavior down to ~30 K and the paramagnetism of the high-spin manganese 3d spins. Band structure calculation of this salt gave an elliptical cylindrical Fermi surface. Because the Fermi surfaces of the adjacent donor layers are rotated to each other by 90°, the θ-$(BETS)_4MnBr_4(EtOH)_2$ salt becomes a two-dimensionally isotropic metal.

Introduction

Recently, the hybrid systems consisting of organic donor molecules and inorganic magnetic anions have attracted much attention of chemists as a possible candidate of bifunctional materials.[1−3] For example, the first paramagnetic organic superconductor, β''-$(BEDT\text{-}TTF)_4(H_2O)[Fe(C_2O_4)_3]$-$(C_6H_5CN)$ [BEDT-TTF = bis(ethylenedithio)tetrathiafulvalene], has received much attention from this viewpoint.[1] More recently, $(BEDT\text{-}TTF)_3[MnCr(C_2O_4)_3]$ has been found to be the first molecular ferromagnetic metal at low temperature.[3] However, in these systems, there is almost no interaction between the magnetic layer of the anions and the conducting layer of the BEDT-TTF molecules. About 10 years ago, we prepared BETS conductors, λ- and κ-$(BETS)_2MCl_4$ [BETS = bis(ethylenedithio)tetraselenafulvalene; M = Ga and/or Fe].[4] In the λ-type salts, we found the systems with superconducting (M = Ga) and $\pi-d$ coupled antiferromagnetic insulating (M = Fe) ground states[5] and the systems exhibiting an unprecedented superconductor-to-insulator

* To whom correspondence should be addressed. E-mail: hayao@ims.ac.jp.
† Institute for Molecular Science.
‡ The University of Tokyo.
§ Institute of Problems of Chemical Physics, RAS.
|| National Institute of Advanced Industrial Science and Technology.

(1) (a) Day, P.; Kurmoo, M. *J. Mater. Chem.* **1997**, *7*, 1291−1295. (b) Graham. A. W.; Kurmoo, M.; Day, P. *J. Chem. Soc., Chem. Commun.* **1995**, 2061−2062. (c) Kurmoo, M.; Graham, A. W.; Day, P.; Coles, S. J.; Hursthouse, M. B.; Caulfield, J. L.; Singleton, J.; Pratt, F. L.; Hayes, W.; Ducasse, L.; Guionneau, P. *J. Am. Chem. Soc.* **1995**, *117*, 12209−12217. (d) Martin, L.; Turner, S. S.; Day, P.; Mabbs, F. E.; McInnes, E. J. L. *Chem. Commun.* **1997**, 1367−1368.
(2) (a) Clemente-León, M.; Coronado, E.; Galán-Mascarós, J. R.; Gómez-García, C. J.; Rovira, C.; Laukhin, V. N. *Synth. Met.* **1999**, *103*, 2339−2342. (b) Ouahab, L. *Coord. Chem. Rev.* **1998**, *178−180*, 1501−1531. (c) Coronado, E.; Gómez-García, C. J. *Chem. Rev.* **1998**, *98*, 273−296.
(3) Coronado, E.; Galán-Mascarós, J. R.; Gómez-García, C. J.; Laukhin, V. N. *Nature* **2000**, *408*, 447−449.
(4) Kobayashi, A.; Udagawa, T.; Tomita, H.; Naito, T.; Kobayashi, H. *Chem. Lett.* **1993**, 2179−2182.

10.1021/ic011160u CCC: $22.00
Published on Web 05/17/2002

transition [M = $Fe_{1-x}Ga_x$ ($x \approx 0.4$)].[6] Furthermore, we have recently discovered a superconducting state under strong magnetic fields ($H > 17$ T) in the λ-$(BETS)_2FeCl_4$ salt. In the $FeCl_4$ system, the coupling of π and d electron systems plays a crucial role to produce the unique antiferromagnetic insulating state which is changed to the metallic state with a ferromagnetic arrangement of Fe^{3+} spins above 11 T[7] and to superconducting state above 17 T.[8] In the κ-type system, we have discovered the antiferromagnetic organic superconductors, κ-$(BETS)_2FeX_4$ (X = Cl and Br), containing magnetic Fe^{3+} anions.[9] The Fe^{3+} spin systems of these salts undergo paramagnetic-to-antiferromagnetic transitions at 0.45 K (X = Cl) and 2.5 K (X = Br) while keeping their metallic states. In addition, these systems undergo a superconducting transition below T_N: 0.17 K (X = Cl) and 1.1 K (X = Br).[9,10] On the other hand, although several BETS salts involving the divalent magnetic anions have been reported so far, their structures and properties have not been clarified except for the θ-$(BETS)_4Cu_2Cl_6$ salt.[11] Recently, we have investigated BETS conductors involving magnetic divalent transition metal halide anions such as $(MX_4)^{2-}$ (M = Co or Mn and X = Cl or Br). Herein, we report the structures and physical properties of these conductors.

Experimental Section

Reagents. BETS was synthesized as described by a method in the literature.[12] The supporting electrolytes of $[(C_2H_5)_4N]_2(MX_4)$ (M = Co or Mn and X = Cl or Br) for the electrocrystallization were prepared by the reaction of $[(C_2H_5)_4N]X$ and $M(II)X_2$ in hot ethanol (EtOH), recrystallized several times from EtOH solution, and dried in vacuo. Chlorobenzene (PhCl) used for elecrocrystallizations was washed three times with concd sulfuric acid and then with aqueous sodium hydrogen carbonate solution and water, followed by drying with calcium chloride and distillation over diphosphorus pentaoxide under nitrogen. EtOH for electrocrystallization was distilled over magnesium ethoxide under nitrogen and stored in refrigerator until use.

Crystallographic Data Collection and Structure Determination. Single-crystal X-ray structure analyses were carried out for the two $(CoCl_4)^{2-}$ salts and the $(MnBr_4)^{2-}$ salt. Data collection for a plate-shaped crystal of the $(CoCl_4)^{2-}$ salt was performed on a Rigaku R-AXIS IV imaging plate area detector with graphite monochromated Mo Kα radiation (λ = 0.71070 Å) at room temperature. Crystal data: black plate, crystal dimensions 0.25 × 0.25 × 0.05 mm^3, $C_{10.5}H_{9.50}S_4Se_4Co_{0.25}ClO_{0.25}$, M = 633.96, orthorhombic, space group *Pccn* (No. 56), a = 8.458(2) Å, b = 35.638(9) Å, c = 11.817(9) Å, V = 3561(2) $Å^3$, Z = 8, ρ_{calcd} = 2.364 g·cm^{-3}, μ = 90.72 cm^{-1}, $F(000)$ = 2386.00. Intensity data were collected to a maximum 2θ value of 51.3° by the ω scan technique. The number of collected reflections was 3396. The data were corrected for Lorentz and polarization effects. The structure was solved by direct method (SHELXS86).[13] The atomic scattering factors were taken from the International Table for X-ray Crystallography.[14] The non-hydrogen atoms except for those of the included solvent molecules were anisotropically refined by full-matrix least-squares method. The isotropic temperature factors were used for the atoms of solvent molecule. Hydrogen atoms were included but not refined. The final cycle of full-matrix least squares refinement was based on 2591 observed reflections [$I > 3.0\sigma(I)$] and 218 variable parameters against $|F|$. R = 0.092, R_w = 0.127, GOF = 3.19. All the calculations were performed using the teXsan crystallographic software package of the Molecular Structure Corporation.[15]

Data collection for block-shaped crystal of the $(CoCl_4)^{2-}$ salt was performed on a Rigaku AFC5R four-circle diffractometer with graphite monochromated Mo Kα radiation (λ = 0.71069 Å) at room temperature. Crystal data: black block, crystal dimensions 0.30 × 0.20 × 0.10 mm^3, $C_{20}H_{16}S_8Se_8CoCl_4$, M = 1345.25, triclinic, space group $P\bar{1}$ (No. 2), a = 12.477(5) Å, b = 16.907(6) Å, c = 8.920(3) Å, α = 93.30(3)°, β = 109.19(3)°, γ = 79.65(3)°, V = 1748(1) $Å^3$, Z = 2, ρ_{calcd} = 2.555 g·cm^{-3}, μ = 96.22 cm^{-1}, $F(000)$ = 1262.00. Intensity data were collected to a maximum 2θ value of 55.0° using the $\omega-2\theta$ scan technique with scan speed of 8.0° min^{-1}. The number of collected reflections was 7950. The data were corrected for Lorentz and polarization effects. An empirical absorption correction based on azimuthal scans of several reflections was applied which resulted in transmission factors ranging from 0.687 to 1.000. The structure was solved by direct method (SHELXS86).[13] The atomic scattering factors were taken from the

(5) (a) Kobayashi, H.; Tomita, H.; Naito, T.; Kobayashi, A.; Sasaki, F.; Watanabe, T.; Cassoux, P. *J. Am. Chem. Soc*. **1996**, *118*, 368−377. (b) Kobayashi, H.; Akutsu, H.; Arai, E.; Tanaka, H.; Kobayashi, A. *Phys. Rev.* **1997**, *B56*, R8526−R8529. (c) Akutsu, H.; Arai, E.; Kobayashi, H.; Tanaka, H.; Kobayashi, A.; Cassoux, P. *J. Am. Chem. Soc*. **1997**, *119*, 12681−12682. (d) Sato, A.; Ojima, E.; Kobayashi, H.; Hosokoshi, Y.; Inoue, K.; Kobayashi, A.; Cassoux, P. *Adv. Mater*. **1999**, *11*, 1192−1194. (e) Tanaka, H.; Kobayashi, A.; Sato, A.; Akutsu, H.; Kobayashi, H. *J. Am. Chem. Soc*. **1999**, *121*, 760−768.

(6) (a) Kobayashi, H.; Sato, A.; Arai, E.; Akutsu, H.; Kobayashi, A.; Cassoux, P. *J. Am. Chem. Soc*. **1997**, *119*, 12392−12393. (b) Sato, A.; Ojima, E.; Akutsu, H.; Kobayashi, H.; Kobayashi, A.; Cassoux, P. *Chem. Lett*. **1998**, 673−674. (c) Kobayashi, H.; Kobayashi, A.; Cassoux, P. *Chem. Soc. Rev*. **2000**, *29*, 325−333.

(7) Brossard, L.; Clerac, R.; Coulon, C.; Tokumoto, M.; Ziman, T.; Petrov, D. K.; Laukhin, V. N.; Naughton, M. J.; Audouard, A.; Goze, F.; Kobayashi, A.; Kobayashi, H.; Cassoux, P. *Eur. Phys. J*. **1998**, *B1*, 439−452.

(8) (a) Uji, S.; Shinagawa, H.; Terashima, T.; Yakabe, T.; Terai, Y.; Tokumoto, M.; Kobayashi, A.; Tanaka, H.; Kobayashi, H. *Nature* **2001**, *410*, 908−910. (b) Balicas, L.; Brooks, J. S.; Storr, K.; Uji, S.; Tokumoto, M.; Tanaka, H.; Kobayashi, H.; Kobayashi, A.; Barzykin, V.; Gor'kov, L. P. *Phys. Rev. Lett*. **2001**, *87*, 7002−7005. (c) Uji, S.; Shinagawa, H.; Terakura, T.; Terashima, T.; Yakabe, T.; Terai, Y.; Tokumoto, M.; Kobayashi, A.; Tanaka, H.; Kobayashi, H. *Phys. Rev*. **2001**, *B64*, 24531−24535.

(9) (a) Ojima, E.; Fujiwara, H.; Kato, K.; Kobayashi, H.; Tanaka, H.; Kobayashi, A.; Tokumoto, M.; Cassoux, P. *J. Am. Chem. Soc*. **1999**, *121*, 5581−5582. (b) Fujiwara, H.; Fujiwara, E.; Nakazawa, Y.; Narymbetov, B. Zh.; Kato, K.; Kobayashi, H.; Kobayashi, A.; Tokumoto, M.; Cassoux, P. *J. Am. Chem. Soc*. **2001**, *123*, 306−314. (c) Otsuka, T.; Kobayashi, A.; Miyamoto, Y.; Kiuchi, J.; Wada, N.; Ojima, E.; Fujiwara, H.; Kobayashi, H. *Chem. Lett*. **2000**, 732−733. (d) Otsuka, T.; Kobayashi, A.; Miyamoto, Y.; Kiuchi, J.; Nakamura, S.; Wada, N.; Fujiwara, E.; Fujiwara, H.; Kobayashi, H. *J. Solid State Chem*. **2001**, *159*, 407−412.

(10) Recently, F. L. Pratt et al. have determined T_c of λ-$(BETS)_2FeCl_4$ to be 0.17 K by μSR experiments (abstract of "The Fourth International Symposium on Crystalline Organic Metals, Superconductors and Ferromagnets", ISCOM 2001, Japan).

(11) (a) Kobayashi, A.; Sato, A.; Arai, E.; Kobayashi, H.; Faulmann, C.; Kushch, N.; Cassoux, P. *Solid State Commun*. **1997**, *103*, 371−374. (b) Kushch, N. D.; Dyachenko, D. A.; Lyubovskii, R. B.; Pesotskii, S. I.; Kartsovnik, M. V.; Kovalev, A. E.; Cassoux, P.; Kobayashi, H. *Adv. Mater. Opt. Electron*. **1997**, *7*, 57−60.

(12) (a) Kato, R.; Kobayashi, H.; Kobayashi, A. *Synth. Met*. **1991**, *41*−*43*, 2093−2096.

(13) Sheldrick, G. M. SHELXS86. In *Crystallographic Computing*, 3rd ed.; Sheldrick, G. M., Kruger, C., Goddard, R., Eds.; Oxford University Press: New York, 1985; p 175.

(14) Cromer, D. T.; Waber, J. T. *International Tables for X-ray Crystallography*; Kynoch Press: Birmingham, England, 1974; vol. 4, Table 2.2A.

(15) *teXsan: Crystal Structure Analysis Package*; Molecular Structure Corporation: The Woodlands, TX, 1985, 1992.

International Table for X-ray Crystallography.[14] The structure was refined by least squares in an anisotropic approximation for all non-hydrogen atoms. The final cycle of full-matrix least squares refinement was based on 3328 observed reflections [$I > 3.0\sigma(I)$] and 370 variable parameters against $|F|$. $R = 0.056$, $R_w = 0.054$, GOF = 1.82. The positions of the hydrogen atoms were found from the geometric conditions and were fixed in the refinement. All the calculations were performed using the teXsan crystallographic software package of the Molecular Structure Corporation.[15]

Data collection for plate-shaped crystal of the $(MnBr_4)^{2-}$ salt was performed on a four-circle diffractometer MXC18 controlled by MXC system (MAC Science) with scintillation counter at room temperature. Mo Kα radiation ($\lambda = 0.71069$ Å) was monochromated by PG(002). Crystal data: black plate, crystal dimensions 0.20 × 0.20 × 0.02 mm^3, $C_{11}H_{11}S_4Se_4Mn_{0.25}BrO_{0.50}$, $M = 688.93$, tetragonal, space group $I4_1/a$ (No. 88), $a = 9.771(4)$ Å, $c = 75.783(5)$ Å, $V = 7235(1)$ Å^3, $Z = 16$, $\rho_{calcd} = 2.530$ g·cm^{-3}, $\mu = 109.49$ cm^{-1}, $F(000) = 5156.00$. Intensity data were collected to a maximum 2θ value of 60.0° by the $\omega-2\theta$ scan technique with scan speed of 8.0° min^{-1}. The number of collected reflections was 5048. The data were corrected for Lorentz and polarization effects. The structure was solved by direct method (SHELXS86).[13] The atomic scattering factors were taken from the International Table for X-ray Crystallography.[14] The non-hydrogen atoms except for those of the solvent were anisotropically refined by full-matrix least-squares method. The isotropic temperature factors were used for the atoms of solvent molecule. Hydrogen atoms were included but not refined. The final cycle of full-matrix least squares refinement was based on 1610 observed reflections [$I > 3.5\sigma(I)$] and 187 variable parameters against $|F|$. $R = 0.068$, $R_w = 0.063$, GOF = 2.98. All the calculations were performed using the teXsan crystallographic software package of the Molecular Structure Corporation.[15]

The measurements of the X-ray photograph at low temperatures were performed using a MAC Science imaging plate system (a rotating anode, Mo Kα) equipped with liquid helium cooling device.

Electrical Resistivity Measurement. The electrical resistivities were measured by the four-probe method along the crystal plane of the single crystals using Huso Electro Chemical System HECS 944C-1 and/or HECS 944C multichannel 4-terminal conductometer. Electrical contacts were achieved with gold wire (15 $\mu m\phi$) and gold paste. The electrical resistivities of the salts except for the two kinds of the $(CoCl_4)^{2-}$ salts were measured down to the liquid helium temperature. Temperature dependence of electrical resistivity of the block-shaped $(CoCl_4)^{2-}$ salt could not be determined because of its insulating nature. The electrical resistivity of the plate-shaped $(CoCl_4)^{2-}$ salt was measured down to 0.7 K. Cooling of samples down to 1.5 K was performed by means of pumping liquid ^{4}He, and the experiments below 1.5 K were performed by means of pumping liquid ^{3}He. Temperature was determined with a calibrated Cerenox thermometer.

Static Magnetic Susceptibility Measurement. Measurement of magnetic susceptibility was carried out using a Quantum Design MPMS-7 SQUID magnetometer in the temperature range from 300 to 2 K at 1 T. The samples were wrapped with a clean aluminum foil whose magnetic susceptibility was separately measured and subtracted. In the case of the plate-shaped κ-$(BETS)_4CoCl_4(EtOH)$, we used sample rotator and measured magnetic susceptibilities on one single crystal by changing the sample orientation in the temperature range from 300 to 6 K at 1 T. The data were corrected for the diamagnetic contribution estimated from the Pascal's constants [$\chi^{dia} = 1.06 \times 10^{-3}$ emu·mol^{-1} for κ-$(BETS)_4CoCl_4$-(EtOH), $\chi^{dia} = 5.58 \times 10^{-4}$ emu·mol^{-1} for $(BETS)_2CoCl_4$, and $\chi^{dia} = 1.13 \times 10^{-3}$ emu·mol^{-1} for the plate-shaped θ-$(BETS)_4MnBr_4$-$(EtOH)_2$].

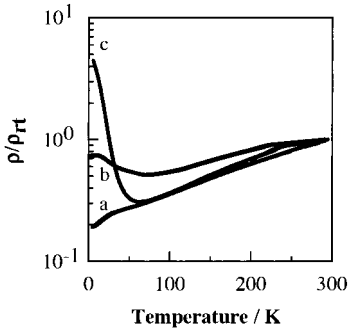

Figure 1. Temperature dependence of electrical resistivities of the divalent anion salts based on the BETS molecule: (a) the plate-shaped $(CoCl_4)^{2-}$ salt, (b) the $(CoBr_4)^{2-}$ salt, and (c) the $(MnBr_4)^{2-}$ salt.

Table 1. Electrical Properties of the Divalent Anion Salts Based on BETS Molecule

anion	shape	electrical properties	σ_{rt}/S·cm^{-1}
$(CoCl_4)^{2-}$	plate	metallic down to 0.7 K	8
$(CoCl_4)^{2-}$	block	insulating	
$(CoBr_4)^{2-}$	plate	metallic down to ∼60 K	4
$(MnBr_4)^{2-}$	plate	metallic down to ∼30 K	58

Band Structure Calculations. The overlap integrals, band structure, and Fermi surface were calculated by a tight-binding method based on the extended Hückel approximation. Slater type atomic orbitals were used for the calculation of molecular orbitals. The parameters of the atomic orbitals are the same as those used in λ- and κ-$(BETS)_2FeCl_4$ salts.[5a] The exponent ζ and the ionization potential (eV) are: Se 4s, 2.112, −20.0; Se 4p, 1.827, −11.0; Se 4d, 1.500, −6.8; S 3s, 2.122, −20.0; S 3p, 1.827, −11.0; S 3d, 1.500, −5.4; C 2s, 1.625, −21.4; C 2p, 1.625, −11.4; H 1s, 1.0, −13.6.

Results and Discussion

Preparation. The BETS salts involving the divalent magnetic anions were prepared by an electrochemical oxidation method in the presence of the corresponding tetraethylammonium salt as a supporting electrolyte under constant current of 0.8 μA in 10% EtOH−PhCl solution at 40 °C for 3−4 weeks. In the case of the electrocrystallization using the supporting electrolyte containing the $(CoCl_4)^{2-}$ anion, two kinds of crystals, namely, plate-shaped and block-shaped crystals, were grown on the anode under identical conditions. The plate-shaped crystals of the $(CoBr_4)^{2-}$ and $(MnBr_4)^{2-}$ salts were also obtained. The X-ray analyses of all the salts except for the $(CoBr_4)^{2-}$ salt were performed, but the structure of the $(CoBr_4)^{2-}$ salt could not be solved because of the bad quality of the crystal.

Electrical Properties. The electrical properties of the obtained salts are summarized in Table 1. Only the block-shaped $(CoCl_4)^{2-}$ salt is an insulator. As shown in Table 1 and Figure 1, the other salts showed comparatively high room-temperature conductivities of the orders of $\sigma_{rt} = 10^0-10^1$ S·cm^{-1}. The resistivities of the $(CoCl_4)^{2-}$, $(CoBr_4)^{2-}$, and $(MnBr_4)^{2-}$ salts decrease from room temperature down to ∼30−60 K, while temperature dependences are relatively small. Below these temperatures, the only plate-shaped $(CoCl_4)^{2-}$ salt keeps stable metallic state down to 0.7 K, and

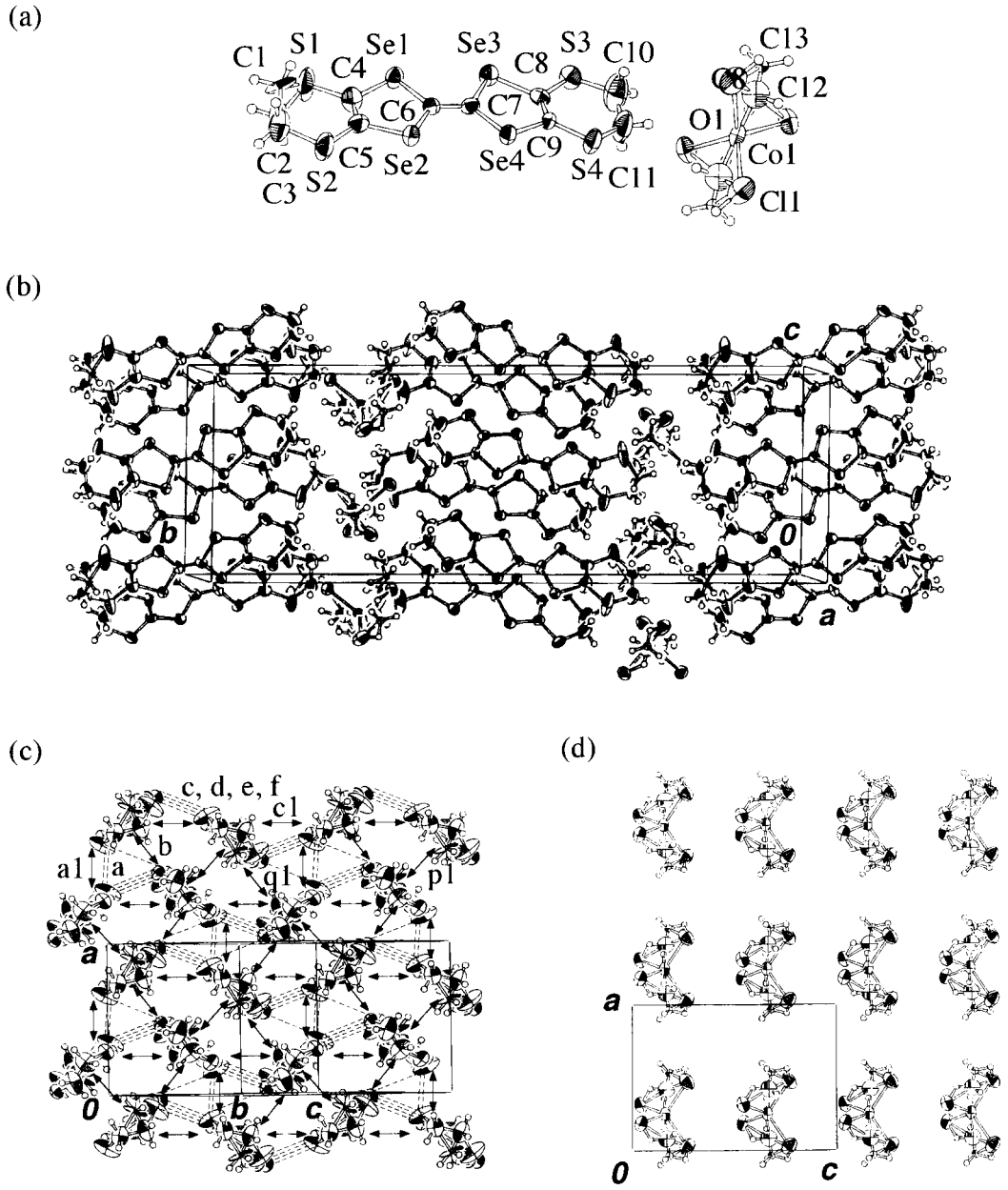

Figure 2. (a) Crystallographically independent molecules of the plate-shaped κ-$(BETS)_4CoCl_4(EtOH)$. (b) Crystal structure of κ-$(BETS)_4CoCl_4(EtOH)$. (c) Donor arrangement and intermolecular contacts of κ-$(BETS)_4CoCl_4(EtOH)$. Intermolecular contacts (Å): (a) S(1)···S(3), 3.426(9); (b) Se(1)···S(4), 3.726(5); (c) S(1)···S(2), 3.41(1); (d) S(3)···S(4), 3.687(7); (e) Se(2)···S(4), 3.650(6); and (f) Se(1)···Se(4), 3.784(3). Overlap integrals: $a1 = -36.17 \times 10^{-3}$, $c1 = -23.00 \times 10^{-3}$, $p1 = 61.19 \times 10^{-3}$, and $q1 = 8.23 \times 10^{-3}$. Intermolecular interplanar distance in a dimer (Å): 3.69. Dihedral angle between dimers (deg): 102.4. (d) Insulating layer containing the anion and solvent molecules of κ-$(BETS)_4CoCl_4(EtOH)$ projected onto the *ac*-plane.

the other salts show slight increases of electrical resistivities. The conducting behavior of the $(CoBr_4)^{2-}$ salt is similar to that of the $(MnBr_4)^{2-}$ salt. Both salts showed small resistivity anomalies around 220−240 K and metal-to-semiconductor transitions around 30−60 K. Therefore, the crystal structure of the $(CoBr_4)^{2-}$ salt is considered to be similar to that of the $(MnBr_4)^{2-}$ salt. We could not observe any superconducting transition in the measured temperature range for these BETS salts containing the divalent magnetic anions.

Crystal Structures. Crystal Structure of the Plate-Shaped $(CoCl_4)^{2-}$ Salt. Figure 2 shows the molecular and crystal structures of the plate-shaped metallic $(CoCl_4)^{2-}$ salt determined at room temperature. There are one independent donor molecule and one-quarter of a crystallographically independent $(CoCl_4)^{2-}$ anion, together with one-quarter of a crystallographically independent EtOH as an interstitial solvent molecule, of which two carbon atoms are positionally disordered (see Figure 2a). The $(CoCl_4)^{2-}$ anions and the disordered EtOH molecules are on a mirror plane and share one crystallographically identical space with 50% probabilities of each other (see Figure 2d). In the anion layer, the shortest Co···Co distances are 5.909(4) Å along the *c*-axis and 8.458(2) Å along the *a*-axis. Between the anion molecules, the shortest Cl···Cl distance along the *c*-axis is 3.83(1) Å [Cl(1)···Cl(2)] and is much shorter than that along the *a*-axis, 4.74(2) Å [Cl(1)···Cl(1)], but these distances are still longer than the sum of the van der Waals radii of chlorines (3.5 Å). There are also several short Cl···S contacts

almost equal to the sum of the van der Waals radii of chlorine and sulfur atoms (3.5 Å) between BETS and the anion molecules. The shortest Cl···S distance is 3.41(1) Å [Cl(1)···S(1)]. These distances are almost the same as those of the antiferromagnetic superconductor κ-$(BETS)_2FeCl_4$.[9] However, long-range magnetic ordering seems to be difficult because the $(CoCl_4)^{2-}$ anions occupy only half of each site. On the other hand, the donors have +0.5 valence because the salt has a 4:1 composition of the donor-to-anion and the $(CoCl_4)^{2-}$ anions are divalent. As shown in Figure 2b, the donors form conducting sheets in the *ac*-plane, which are separated from each other by sheets of the anions and the EtOH solvents along the *b*-axis. The donors have the conventional κ-type two-dimensional arrangement in the conducting sheet (see Figure 2c). Interplanar distance within the dimer is 3.69 Å, and the dihedral angle between the dimers is 102.4°. The analysis of BETS intermolecular distances shows that there is no short contact in the dimer, but there are many short interdimer contacts (see caption of Figure 2) mediated by the sulfur and selenium atoms less than the sum of the van der Waals radii. These short contacts form the two-dimensional network in the donor layers and yield the metallic conducting properties of this salt.

Crystal Structure of the Block-Shaped $(CoCl_4)^{2-}$ Salt. As Figure 3a indicates, an X-ray analysis of the block-shaped insulating $(CoCl_4)^{2-}$ salt revealed that there are two crystallographically independent donor molecules (A and B) and one crystallographically independent $(CoCl_4)^{2-}$ anion. Each BETS molecule is in a monocationic state because this salt has a 2:1 composition of donor-to-anion. The donors stack along the *c*-axis and strongly dimerize in an almost eclipsed configuration as shown in Figure 3c. On the other hand, the $(CoCl_4)^{2-}$ anions are located between the donor stacks in "chessboard" fashion (see Figure 3b). The shortened contacts mediated by the sulfur and selenium atoms exist between the interstack donors and those in the dimer (see caption of Figure 3). There are also many contacts between donors and anions, suggesting the strong interaction between the donors and anions, as is indicated by the dotted lines in Figure 3b. However, there is no direct interaction between the anions because the anion array along the *c*-axis is completely separated by the donor columns and the shortest Co···Co distance along the *c*-axis is the very long value of 8.920(3) Å, suggesting the weak interaction between the cobalt spins. Although there are many shortened contacts between the donors less than the sum of the van der Waals radii, the block-shaped $(CoCl_4)^{2-}$ salt is an insulator because of its dimerized stacks of the monocationic BETS molecules.

Crystal Structure of the $(MnBr_4)^{2-}$ Salt. Figure 4 shows the molecular and crystal structures of the $(MnBr_4)^{2-}$ salt. The donor-to-anion ratio is 4:1, and donors have +0.5 valence. Two independent halves of the donors (A and B in Figure 4a) lie on the 2-fold axis and the inversion center, respectively (see Figure 4a). As Figure 4b indicates, the donor layers alternate with the anion−solvent layers along the *c*-axis. Figure 4c shows that the −A−A′−A− and −B−B′−B− stacks arrange alternately to each other and form the two-dimensional donor layers in the *ab*-plane.

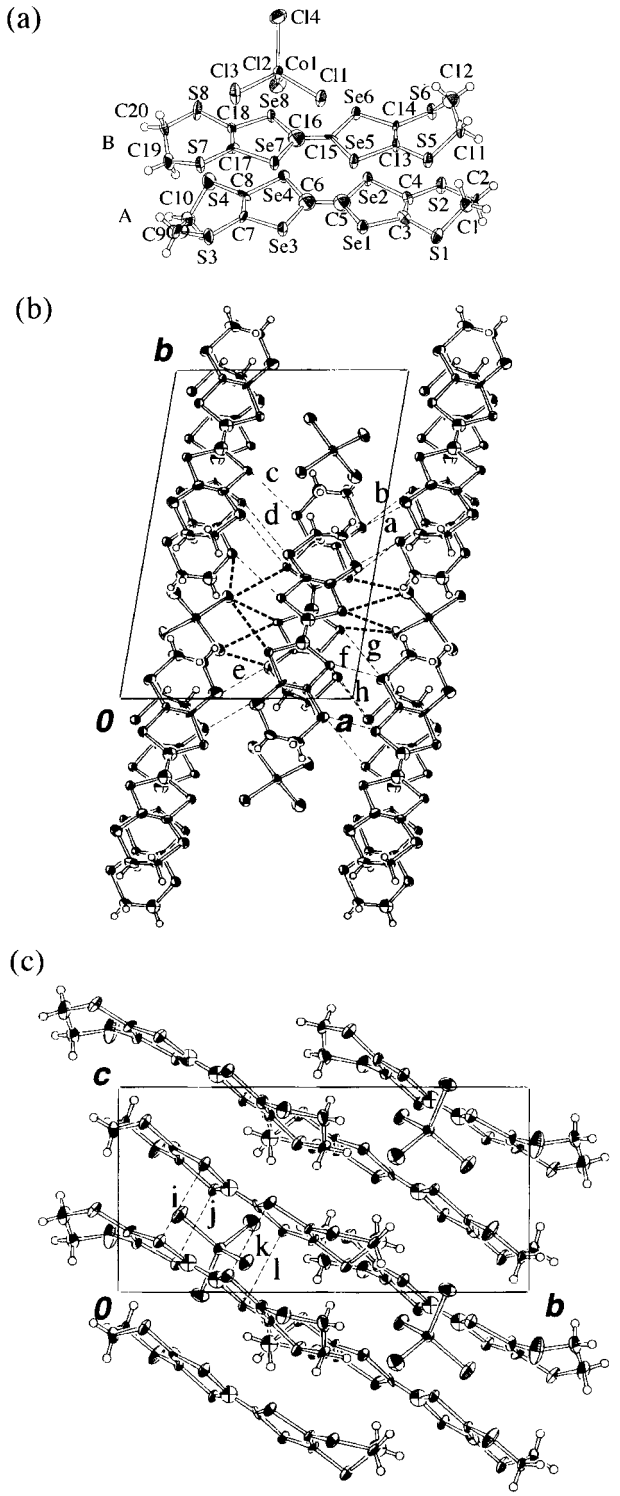

Figure 3. (a) Crystallographically independent molecules of the block-shaped $(BETS)_2CoCl_4$. (b) Crystal structure of $(BETS)_2CoCl_4$ projected onto the *ab*-plane. Intermolecular contacts between the donor columns (Å): (a) S(1)···S(5), 3.469(7); (b) Se(5)···S(5), 3.538(5); (c) Se(2)···S(6), 3.387-(6); (d) Se(6)···S(2), 3.593(6); (e) S(4)···S(8), 3.202(8); (f) Se(3)···S(3), 3.525(6); (g) Se(7)···S(3), 3.465(6); and (h) Se(3)···S(7), 3.642(6). (c) Donor columns of $(BETS)_2CoCl_4$ projected onto the *bc*-plane. Intrastack intermolecular contacts (Å): (i) Se(3)···Se(7), 3.694(3); (j) Se(4)···Se(8), 3.418-(3); (k) Se(1)···Se(5), 3.536(3); and (l) Se(2)···Se(6), 3.516(3).

Intermolecular interplanar distances are 3.89 Å for the A−A′ molecules and 3.93 Å for the B−B′ molecules with the slip distances of 3.09 and 0.03 Å along the molecular long axis

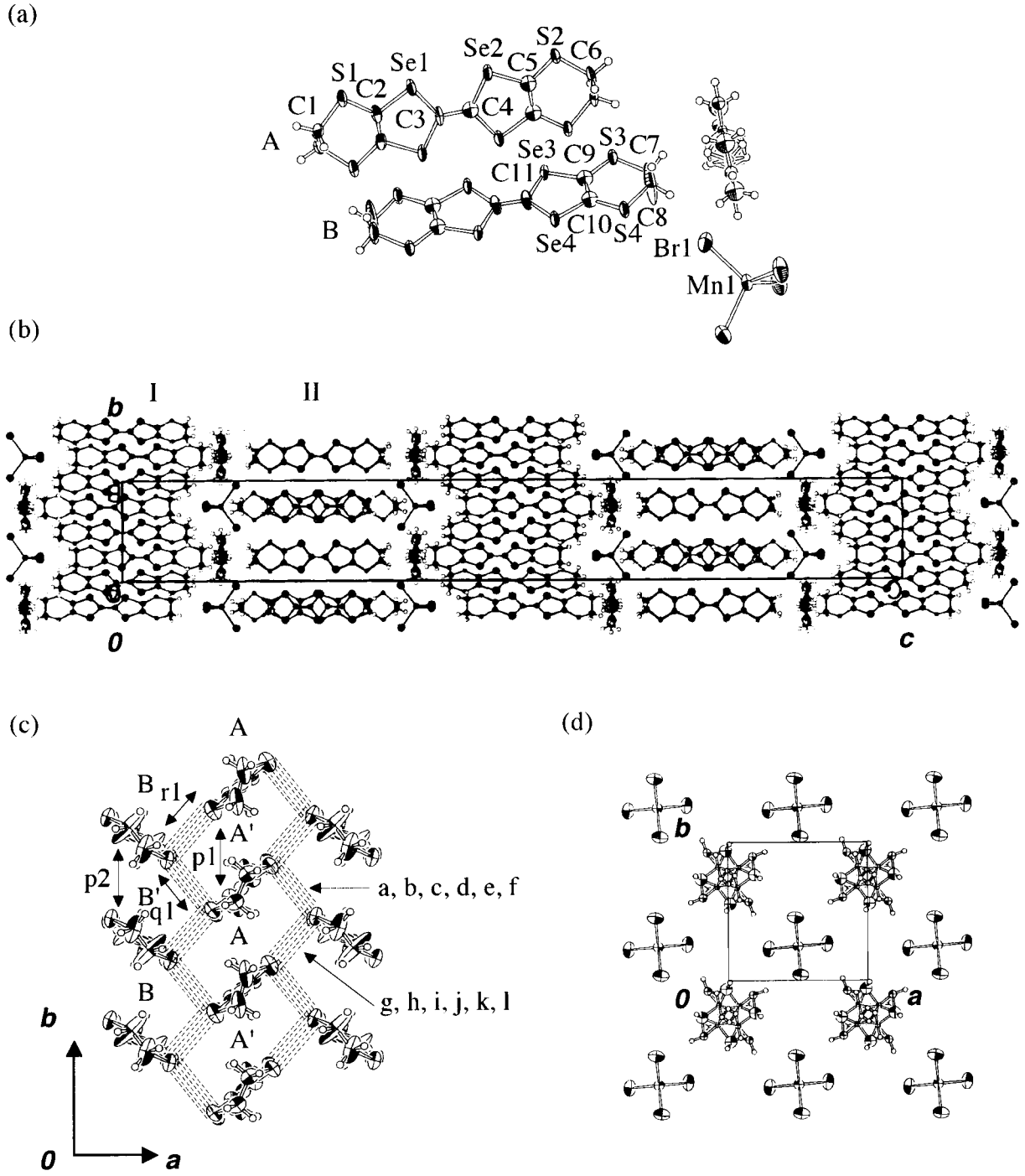

Figure 4. (a) Crystallographically independent molecule of the plate-shaped θ-$(BETS)_4MnBr_4(EtOH)_2$. (b) Crystal structure of θ-$(BETS)_4MnBr_4(EtOH)_2$. (c) Donor layer and intermolecular contacts of θ-$(BETS)_4MnBr_4(EtOH)_2$. Intermolecular contacts (Å): (a) S(1)···Se(3), 3.583(6); (b) S(2)···S(4), 3.507(6); (c) S(2)···Se(4), 3.561(5); (d) S(3)···Se(1), 3.717(5); (e) Se(1)···Se(3), 3.735(3); (f) Se(2)···Se(4), 3.710(3); (g) S(1)···S(4), 3.671(6); (h) S(2)···S(3), 3.592-(6); (i) S(2)···Se(3), 3.675(5); (j) S(4)···Se(1), 3.553(5); (k) Se(1)···Se(4), 3.736(2); and (l) Se(2)···Se(3), 3.746(3). Overlap integrals: $p1 = 4.83 \times 10^{-3}$, $p2 = 3.31 \times 10^{-3}$, $q1 = -43.36 \times 10^{-3}$, and $r1 = -42.83 \times 10^{-3}$. Intermolecular interplanar distance (Å): 3.89 for the −A−A′−A− donor array and 3.93 for the −B−B′−B− donor array. Dihedral angle between donor molecules of the adjacent stacks (deg): 102.4. (d) Insulating layer containing the anion and solvent molecules of κ-$(BETS)_4MnBr_4(EtOH)_2$ projected onto the *ab*-plane.

and the large slip distances of 2.95 and 2.89 Å along the molecular short axis, respectively. The dihedral angle of the donors between the neighboring stacks is 102.9°. The arrangement of the donor molecules is parallel to each other in the uniform stacks and is so-called θ-type donor array. On the other hand, the manganese atoms are located on the special position of $\bar{4}$ center. In addition, the EtOH molecules are beside the anions and occupy the crystallographic void spaces as the interstitial solvents (see Figures 4d). The solvents also exist around $\bar{4}$ center and are disordered. Both the $(MnBr_4)^{2-}$ anions and disordered solvent molecules form the anion−solvent layers in the *ab*-plane. Figure 4b shows that there are two types of donor layers (I and II). In the first type of layer, the donor molecules form the stacks along

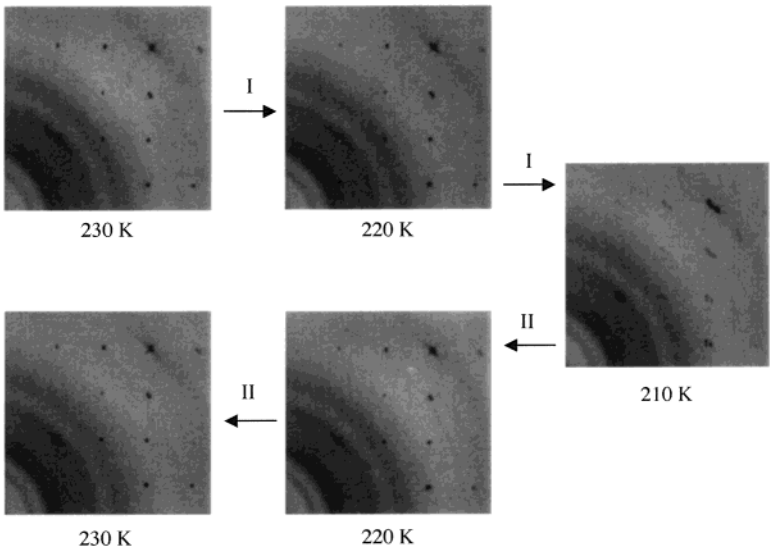

Figure 5. Temperature dependence of the X-ray photograph of θ-$(BETS)_4MnBr_4(EtOH)_2$ in the temperature range of 210−230 K. I and II denote cooling and warming steps, respectively.

the *b*-axis (layer I), while in the second type of layer the stacks lie down along *a*-axis (layer II). Namely, the donors stacked with rotating their stacking axis with an angle of 90° between the adjacent donor layers. These layers arrange alternately along the *c*-axis such as −I−II−I−II− order, which explained the large unit cell parameter *c* [75.783(5) Å] (see also Figure 4b). Such a similar structure with the −I−II−I−II− order and θ-type donor arrangement is already known in θ-$(BETS)_4HgBr_4(PhCl)_x$, where $x \approx 0.25$.[16] Although no intermolecular contact is found in each stack because of large intermolecular interplanar distance and large slip distance along the molecular short axis, there are many shortened contacts between the donors of the neighboring stacks as shown in Figure 4c (see caption of Figure 4). Therefore, two-dimensional networks are developed in the donor layers. With respect to the anion layer, the shortest Mn···Mn distance is the very long value of 9.77 Å because of its anion−solvent mixed structure, and there is only one contact between the donor and anion [Br(1)···S(3), 3.926(5) Å], suggesting its weak interaction between the donor and anion layer.

The temperature dependence of the X-ray photograph of the $(MnBr_4)^{2-}$ salt in the temperature range of 210−230 K is shown in Figure 5, where changes of the X-ray photograph at cooling and warming cycles are presented. Figure 5 displays the presence of some structural anomalies in the temperature range 210−220 K, where a resistivity anomaly was observed. In the cooling run, there was no change in the temperature range 220−230 K; however, each single spot at 220 K separated to several ones at 210 K. Furthermore, the separated spots returned to the original single spots at 220 K in the warming run. The results indicate the presence of the structure transformation of the $(MnBr_4)^{2-}$ salt in the temperature range 210−220 K, and the anomaly of the resistivity curve at 220 K is considered to be derived from some structural changes. The studies on the crystal structure analyses at low temperatures are now in progress, and the details will be reported elsewhere.

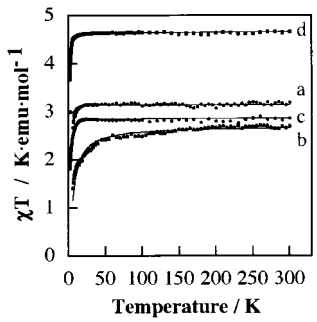

Figure 6. Temperature dependence of the χT value at 1 T of the single crystal of the plate-shaped κ-$(BETS)_4CoCl_4(EtOH)$ measured (a) perpendicular to the *c*-axis ($\chi_\perp T$) and (b) parallel to the *c*-axis ($\chi_{||} T$) and the polycrystalline sample of (c) the block-shaped $(BETS)_2CoCl_4$ and (d) the plate-shaped θ-$(BETS)_4MnBr_4(EtOH)_2$. The fitting curves for (a) and (b) are calculated based on the values $D = 4$ K, $g_{||} = 2.4$, $g_\perp = 2.6$, and $\theta = -1.5$ K. The fitting curve for (c) is calculated as a averaged one on the basis of the values $D = 4$ K, $g_{||} = 2.4$, $g_\perp = 2.6$, and $\theta = -0.5$ K. The fitting curve for (d) is calculated from the Curie−Weiss law ($C = 4.7$ K emu mol^{-1} and $\theta = -0.3$ K).

Magnetic Properties. Magnetic susceptibilities were measured on one single crystal of the plate-shaped $(CoCl_4)^{2-}$ salt and polycrystalline samples of the block-shaped $(CoCl_4)^{2-}$ salt and the $(MnBr_4)^{2-}$ salt using SQUID magnetometer at 1 T. To analyze the results of the SQUID measurements, we neglect the contribution from the cation radical spins, because they are always very small and much less than the 10% of the value for the high-spin cobalt and manganese spins even at room temperature. Figure 6 shows the temperature dependence of the χT values of these salts. In the plate-shaped $(CoCl_4)^{2-}$ salt, we measured the angular dependence of the magnetic susceptibilities on one single crystal at 10 K and observed clear anisotropy of the magnetic properties. The minimum of the susceptibilities ($\chi_{||}$) was observed when the field was applied parallel to the *c*-axis. On the other hand, maxima ($\chi_\perp$) were observed when the magnetic field was applied perpendicular to the *c*-axis; namely, the direction for $\chi_\perp$ includes directions parallel to

(16) Naito, T.; Miyamoto, A.; Kobayashi, H.; Kato, R.; Kobayashi, A. *Chem. Lett.* **1991**, 1945−1948.

the *a*-axis and the *b*-axis, suggesting an axial magnetic anisotropy. Then, we measured the temperature dependence of the magnetic susceptibilities for the directions $\chi_{\parallel}$ and $\chi_{\perp}$. As shown in Figure 6, they indicated clear differences and decreases of the χT values. They could be fitted by introducing both the zero-field splitting parameter D of $S = {}^3/_2$ localized spin system and small Weiss temperature when adopting the values $D = 4$ K, $g_{\parallel} = 2.4$ and $g_{\perp} = 2.6$, and $\theta = -1.5$ K.[17] The difference of the *g*-values is considered to originate from the anisotropic nature of the *g*-tensor of the tetrahedral cobalt tetrachloride anion,[18] and the small Weiss temperature suggests the existence of an weak short-range antiferromagnetic interaction between the neighboring cobalt tetrachloride anions in the disordered anion layer. On the other hand, in the case of block-shaped $(CoCl_4)^{2-}$ salt, we also observed a decrease of the χT value in the low-temperature region. However, this measurement was performed on many pieces of block-shaped crystal, and the obtained χT curve almost corresponds to the averaged one calculated from the same zero-field splitting parameter and *g*-values as the former plate-shaped $(CoCl_4)^{2-}$ salt and smaller Weiss temperature ($\theta = -0.5$ K) [$\chi T = (\chi_{\parallel} T + 2 \times \chi_{\perp} T)/3$] as shown in Figure 6. On the other hand, the temperature dependence of magnetic susceptibilities of the $(MnBr_4)^{2-}$ salt showed the Curie constant ($C = 4.7$ K·emu·mol^{-1}), which is approximately equal to 4.38 K·emu·mol^{-1} expected for the $S = {}^5/_2$ localized spin system with $g = 2.0$ and almost zero Weiss temperature ($\theta = -0.3$ K) within an experimental error, suggesting the absence of the interaction between the manganese ions. These results indicate that the magnetic interactions between the high-spin cobalt or manganese 3d spins are very weak or almost absent because of the jumbled structures by the anion molecules and the solvents or the donor molecules. Furthermore, we could not observe any anomalies of the magnetic susceptibilities corresponding to the resistivity anomalies in these salts.

Calculated Band Structures. Band Structure of the Plate-Shaped $(CoCl_4)^{2-}$ Salt. The band structure of the plate-shaped $(CoCl_4)^{2-}$ salt was calculated by the tight-binding method based on the extended Hückel approximation. The calculated overlap integrals are $p1 = 61.2 \times 10^{-3}$ in the dimer and $q1 = 8.23 \times 10^{-3}$, $a1 = -36.2 \times 10^{-3}$, and $c1 = -23.0 \times 10^{-3}$ between the dimers (see Figure 2c). As shown in Figure 2c, the overlap integral between the donor molecules arranged parallel ($p1$) are twice or three times larger than those between the donor molecules perpendicularly arranged ($a1$ and $c1$). Large intradimer overlap integrals indicate a strong dimerization in the donor layer. Because of this strong dimerization, the upper two bands and lower ones are completely separated (see Figure 7). The energy gap is 0.36 eV. The band dispersion is degenerated on the ZV zone boundary as a result of the existence of a *c*-glide plane. The Fermi surface is essentially two-dimensionally cylindrical. The stable metallic state of this $(CoCl_4)^{2-}$ salt is attributable to the two-dimensionality of the band structure.

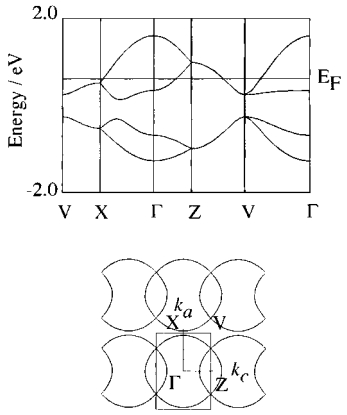

Figure 7. Calculated band structure and Fermi surface of the plate-shaped κ-$(BETS)_4CoCl_4(EtOH)$. Mid-gap between the upper two branches and the lower two branches is 0.36 eV, and bandwidth of the upper band is 1.54 eV.

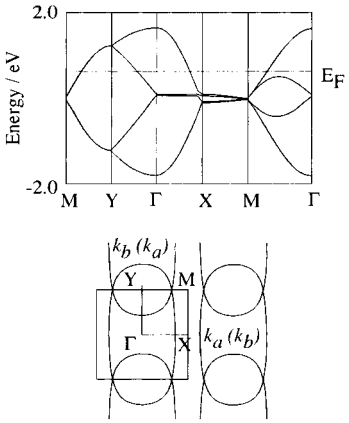

Figure 8. Calculated band structure and Fermi surface of the plate-shaped θ-$(BETS)_4MnBr_4(EtOH)_2$.

Band Structure of the $(MnBr_4)^{2-}$ Salt. Band structure calculation was also carried out on the donor layer I of the $(MnBr_4)^{2-}$ salt. As Figure 4c indicates, the calculated overlap integrals are $p1 = 4.83 \times 10^{-3}$ and $p2 = 3.31 \times 10^{-3}$ in the stack and $q1 = -43.36 \times 10^{-3}$ and $r1 = -42.83 \times 10^{-3}$ between the stacks, respectively. The intrastack overlap integrals are very much smaller than the interstack overlaps. Therefore, intermolecular interactions are strong along the diagonal direction in the *ab*-plane. As shown in Figure 8, the Fermi surface derived from these overlap integrals is a two-dimensional elliptical cylinder and closed in the MY boundary as a result of space group symmetry. The stable metallic state of the $(MnBr_4)^{2-}$ salt is attributable to the two-dimensionality of the band structure. As mentioned before, the adjacent donor layers are arranged with the rotating angle of 90° to each other. Inevitably, the calculated Fermi surface for the neighboring donor layer is also revolved as well. Hence, the $(MnBr_4)^{2-}$ salt is considered to be an isotropic two-dimensional metal. However, we observed a slight increase of the resistivity below 30 K. We consider that there is structural transition around 210−220 K, where a resistivity anomaly was observed, Fermi surfaces are subjected to some

(17) Boca, R. *Theoretical Foundations of Molecular Magnetism*; Elsevier Science: Lausanne, Switzerland, 1999; p 437.

(18) (a) Shankle, G. E.; McElearney, J. N.; Schwartz, R. W.; Kampf, A. R.; Carlin, R. L. *J. Chem. Phys.* **1972**, *56*, 3750−3758. (b) Mori, H.; Sakurai, N.; Tanaka, S.; Moriyama, H. *Bull. Chem. Soc. Jpn.* **1999**, *72*, 683−689.

changes of their shapes, and a slight instability of metallic state may happen.

Conclusion

We prepared several metallic divalent anion salts based on the BETS molecule by electrocrystallization by using the supporting electrolytes containing tetrahedral anions such as $(MX_4)^{2-}$ (M = Co or Mn and X = Cl or Br). With regard to the $(CoCl_4)^{2-}$ salt, two types of crystals were obtained. One of them, the plate-shaped crystal, was determined to be κ-$(BETS)_4CoCl_4(EtOH)$. Temperature dependence of the electrical resistivity indicated metallic behavior down to 0.7 K. No signature of a superconducting transition was obtained. The magnetic measurement of κ-$(BETS)_4CoCl_4(EtOH)$ indicates that there is clear anisotropy of the temperature dependence of magnetic susceptibilities caused by zero-field splitting and is only very weak antiferromagnetic interaction between cobalt 3d spins of $S = {}^3/_2$, probably because both the anion and solvent molecules populate disorderly with 50% probabilities. The other salt, $(BETS)_2CoCl_4$, is an insulator because of the monocationic state and the dimerized structure of BETS. On the other hand, the $(MnBr_4)^{2-}$ salt has the θ-type donor array. In the crystal, the donor stacking directions are rotated with an angle of 90° between the adjacent donor layers separated by the anion/solvent layer. This θ-$(BETS)_4MnBr_4(EtOH)_2$ salt showed metallic conducting behavior down to ~30 K, below which resistivities increased slightly. The magnetic properties of this salt indicated the paramagnetism of the high-spin manganese 3d spins. We succeeded in the preparation of the several metallic salts based on the BETS molecules and divalent tetrahedral magnetic anions, but the magnetic interaction between the localized magnetic moments was revealed to be very weak or almost absent because of the incorporation of the solvent in the anion layers. The preparation of magnetic divalent anion salts with 4:1 composition of the donor-to-anion without solvent molecule will be highly desired.

Acknowledgment. This work is financially supported by a Grant-in-Aid for Scientific Research on Priority Areas (B) of Molecular Conductors and Magnets (11224101 and 11224211) from the Ministry of Education, Science, Sports and Culture, Japan.

Supporting Information Available: Three X-ray crystallographic files, in CIF format. This material is available free of charge via the Internet at http://pubs.acs.org.

IC011160U